Please fill in the name of the event you are preparing this manuscript for.	SPE Middle East Oil & Gas Show and Conference
Please fill in your 6-digit SPE manuscript number.	SPE-195046-MS
Please fill in your manuscript title.	Enhancing the near-surface image using duplex-wave reverse time migration

Please fill in your author name(s) and company affiliation.

Given Name	Surname	Company
Ghada	Sindi	Saudi Aramco
Tariq	Alkhalifah	KAUST
Tong	Fei	Saudi Aramco
Yi	Luo	Saudi Aramco

Abstract

Reverse time migration (RTM) involves zero-lag cross-correlation of forward extrapolated source function wavefields and backward extrapolated receiver wavefields. For a near surface with complex structures and velocity anomalies, forward propagating the source wavelet generates wavefields containing reflections, near-surface multiples, and scattered direct arrivals. The wavefields are recorded as upgoing arrivals contaminated by the same reflections, near-surface multiples, and scattered signals, which can be critical for imaging near-surface structures and scatterers.

Here, we develop a new depth migration, duplex reverse time migration (DRTM) technique to improve imaging of complex near-surface structures. DRTM uses the direct arrival as a source to forward propagate and generate source wavefields, and reversely extrapolated recorded data in a zero-lag cross-correlation imaging condition to generate the final section. The interaction between the data components during cross-correlation can use primaries and multiples to image the near-surface structure correctly. Cross-talk artifacts may exist, but they are comparatively weak.

DRTM is demonstrated on both synthetic and field data examples showing an enhanced image in areas with complex near-surface structures compared to conventional RTM imaging methods. The new algorithm can significantly enhance shallow imaging without additional computation costs compared with conventional RTM. It can produce an image with higher resolution and signal-to-noise (S/N) ratio by replacing the source wavelet with the recorded direct arrivals, which include near-surface information necessary to boost the image in areas with near-surface complexity. Since the direct arrivals are one of the most energetic events recorded, the resultant image is typically of high S/N. The wave can also illuminate shallow zones better than primaries in marine environments.

Introduction

Over recent decades, advancements in computational power have made reverse time migration (RTM) popular for seismic imaging (Baysal et al., 1983; McMechan, 1983). Unlike the Kirchhoff approach, RTM does not need to honor the high-frequency approximation. Therefore, it is capable of illuminating arbitrarily complicated regions such as subsalt without any dip limitations or shadow zones. RTM still struggles to image near-surface reflectors. To mitigate this issue, we propose to incorporate duplex waves in the RTM algorithm.

In general, time-domain RTM involves three steps: downward continuation of the source wavefield (forward in time), downward continuation of the receiver wavefield (backward in time), followed by an application of an imaging condition, often a zero-lag cross-correlation of those computed wavefields. Before backward propagated the wavefields, we require to preprocess observed data to filter out unwanted events such as direct arrivals, diving waves, and multiples that would otherwise result in false events in the image. To incorporate multiples along with primary events, Liu et al. (2011) modified conventional RTM to image multiple reflections to their correct locations in the subsurface. Multiples can be imaged by forward propagating primaries as shown by Berkhout and Verschuur (1994). Alkhalifah and Zuberi (2011) modified conventional RTM to get better illumination beneath the near surface.

Forward propagating the recorded data was studied by Alkhalifah and Zuberi (2011). They found that direct arrivals play an essential role in improving the image, using both the primaries and multiples. Data recorded on the surface include direct arrivals (*D*), primary reflections (*P*) and multiples (*M*). In this work, instead of forward propagating the source function or recorded data (Alkhalifah and Zuberi, 2011), we propose to forward extrapolate direct arrival wavefields and backward recorded data wavefields, then apply the zero-lag cross-correlation imaging condition.

Forward propagation of the actual source is equivalent to the forward propagation of the direct arrivals in inhomogeneous media (Zuberi and Alkhalifah, 2013). As a result, there is an interaction between the forward propagation of the direct arrivals and backward propagation of the primaries that is similar to conventional RTM. Instead of utilizing the forward propagation of the source, we can replace it and utilize forward propagation of the direct arrivals. The cross-correlation imaging condition was used by Zhang et al. (2007), who showed that forward propagation of the recorded data included additional cross-talk noise, some of which does not occur in conventional RTM. The relative cross-talk noise amplitudes were reduced as a result of the summation of the two amplitudes coming from the primaries and the multiples. It is important to note that this sort of cross-talk can be suppressed by adjusting the deconvolution imaging condition for laterally heterogeneous media (Muijs et al., 2007).

The strongest events in the recorded data are often the direct arrivals. These are assumed to be the source of the majority of the energy used in imaging. We show in this abstract that we can use the direct arrivals as the source for forwarding propagation to get a wavefield roughly equivalent to that of the source. The input for the new RTM scheme involves forward propagating the direct arrivals, which creates the source wavefield containing information on the near-surface scattering and velocity variations.

In this abstract, we apply the approach of forward propagating the direct arrivals using a two-layer model, including velocity anomalies, as well as on the Marmousi model. Finally, we demonstrate the algorithm on a 2D field data example.

Theory

The following equations are given in the frequency domain, and the time-periodic factor is neglected. The final image results from summation over frequency.

Let us assume A is a matrix representing a shot gather. A includes direct arrivals, primaries, and multiples, and is given by:

$$A = D + P + M. \qquad (1.1)$$

where D is the direct arrivals, P is primaries, and M first-order multiples. The directional derivatives (normal to the surface) are given by:

$$D' = \frac{\partial D}{\partial n}, P' = \frac{\partial P}{\partial n}, etc. \qquad (1.2)$$

Forward propagation of the direct arrivals can be written as:

$$GA' = GD'. \qquad (1.3)$$

and backward propagation of the recorded data can be written as:

$$G^*A' = G^*D' + G^*P' + G^*M', \qquad (1.4)$$

where G is the Green's function, and $G^*$is a complex conjugate. Let $s(x, \omega)$ be a point source, then $p(x, \omega)$ is the pressure waveeld, and $s(x, \omega) = \delta(x)f(x)$ a column matrix S. Furthermore, we will prove this equation:

$$GD' \sim p(x, \omega) \equiv GS. \qquad (1.5)$$

By applying the zero-lag cross-correlation imaging condition between equations (1.3) and (1.4), we obtain an image I_{AA}:

$$I_{AA} = G(D')(G^*(D' + P' + M'))^*$$

$$= G(D')(G^*(P' + M'))^* + G(D')(G^*D')^* \qquad (1.6)$$

$$= \underbrace{(GD')(G^*P')^*}_{\text{Imaging Primaries}} + CTK,$$

where the cross-talk terms are represented by CTK (Zuberi and Alkhalifah, 2013). In contrast, conventional RTM is given by:

$$I_{SA} = GS(G^*(D' + P' + M'))^*$$

$$= (GS)(G^*P')^* + (GS)(G^*M')^*. \qquad (1.7)$$

$$\underbrace{(GS)(G^*P')^*}_{\text{Imaging Primaries}} \quad \underbrace{(GS)(G^*M')^*}_{\text{Cross-talk terms}}$$

G^*D' can be ignored, since it does not penetrate the earth and so they cannot be used to image the subsurface. Equation (1.6) shows that the image can be obtained by forward propagating the direct arrivals so that we can image primaries. To show all results, equation (1.6) will be expanded as:

$$I_{AA} = I_{DP} + I_{DM}$$

$$= (GD')(G^*P')^* + (GD') + (G^*M')^*. \qquad (1.8)$$

For the first term in equation (1.8), Zuberi and Alkhalifah (2013) showed that forward propagating the direct arrivals from the seismic data is roughly equivalent to forward propagating the actual source $GS \approx GD'$:

1. $I_{DP} = (GD')(G^*P')$: This term will image the primaries. The direct-primary part is equivalent to the internal-crosstalk RTM, shown by Zuberi and Alkhalifah (2013).

2. $I_{DM} = (GD')(G^*M')$: This term gives the noise. It is a result of the interaction between the forward propagating direct arrivals and the back propagating multiples. This noise is in conventional RTM (Zuberi and Alkhalifah, 2013), as well.

Limitations

There are some limitations when forward propagating the direct arrivals. First, the receiver coverage should be dense enough to avoid aliasing, for example, in the numerical experiments below the spacing is 25 m for seismic recording. Second, the near-offset (particularly the zero offset) traces should be recorded in the data. If we are forward propagating the recorded data, we should change the sign of the direct arrivals to image the primaries and multiples simultaneously, and this demands an extra processing step.

1. Near-Offset (Zero-Offset) Recorded

According to Huygens principle, any point on the wavefront may be considered as a source. The first Fresnel zone contributes to, and the minimum traveltime path recreates, the wavefront. If the source is located on the surface, then the path from the source to itself is the minimum traveltime path. Consequently, we require the traces that occur inside the first Fresnel zone surrounding the zero offset to generate the direct arrival wavefield. Figure 1 shows the impact of neglecting the near-offsets. The difference is clear between the two-wavefield snapshots. We solve the missing near-offset issue by using interferometry to interpolate the missing near-offset traces.

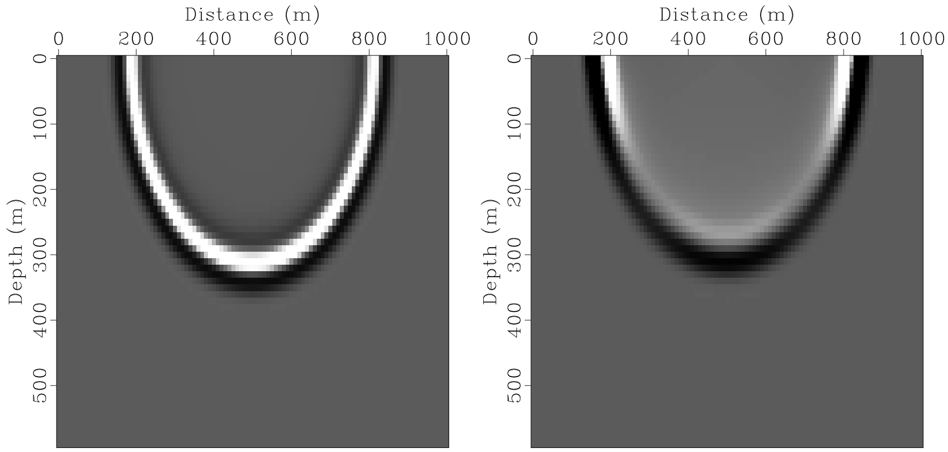

(a) **(b)**

Figure 1 – Wavefield snapshot, (a) wavefield from source function on the surface, (b) wavefield using direct arrival missing 20 near-offset traces.

2. Direct Arrival and Reversing the Polarity

In theory, we know that the polarity of the primary reflection and direct arrivals should be the same. When we image primaries and multiples, they will cancel each other out unless the primary reflection and the direct arrival have opposite polarity (Verschuur and Berkhout, 2011; Zuberi and Alkhalifah, 2013).

Seismic Imaging Methods:

1. Conventional Reverse Time Migration RTM

Conventional RTM utilizes the zero-lag cross-correlation imaging condition applied to the forward extrapolated source function and the backward extrapolated receiver wavefields (Koslo and Baysal, 1983; McMechan, 1983). Figure 2(a) shows typical raypaths of arrivals used in conventional reverse time migration. *S* represents the source position, *R* represents the receiver, and *A* is the scattering point.

2. Seismic Imaging Using Surface Multiples

Surface multiples are waves that are reflected at least once at the surface and end up at the receivers as in Figure 2(b). S_o, *A*, and *B* are scattering points. Multiples take a longer wave path and cover larger regions than primary waves in the medium (Davydenko and Verschuur, 2017; Kumar* et al., 2014). During imaging using surface multiples, we replace the source function by recorded data that includes primaries and multiples on the surface, and then we replace the primary reflection by multiples. To get the image, we forward extrapolate in time the primaries and multiples recorded on the surface and backward extrapolate in time multiples recorded on the surface. We then apply the imaging condition (Liu et al., 2011).

3. Seismic Imaging Using Internal Multiples

Internal multiples are often generated within salt domes, coal beds, basalt layers, and other geologic structures with high-velocity contrasts, as shown in Figure 2(c). *S* represents the source position, and *R* represents the receiver. *A*, *B*, and *C* are the scattering points. Imaging using internal multiples is based on decomposing the extrapolated source function and receiver wavefields into up- and downgoing wavefields. Then the imaging condition is applied to these decomposed wavefields (Liu et al., 2015).

4. Imaging Using Duplex Waves

Duplex-wave reverse time migration (DRTM) uses the direct arrival as a source to forward propagate and generate source wavefields, reversely extrapolates the recorded data, and applies the zero-lag cross-correlation imaging condition. Figure 2(d) shows the DRTM wave path using *S* as the source location. *R* is the receiver location, and *A* is the scattering point.

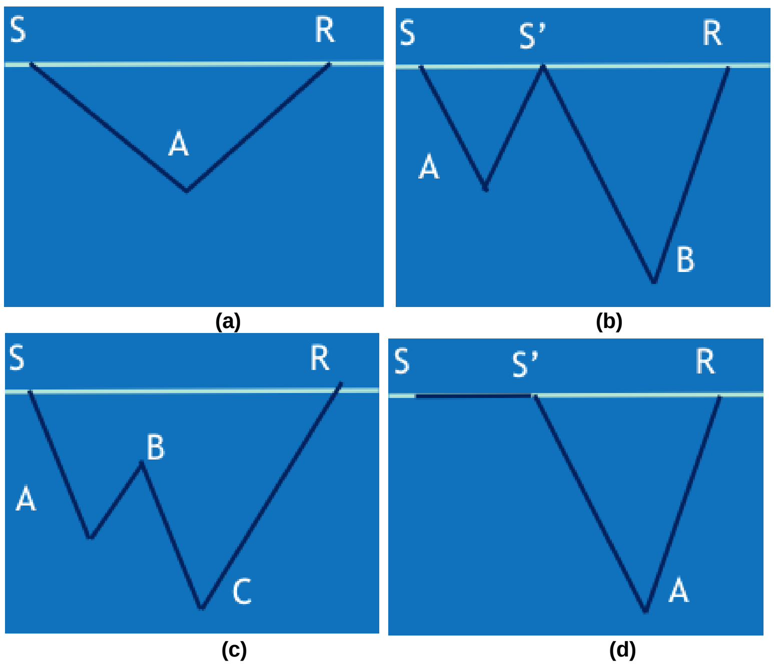

Figure 2 – Raypath diagrams for different arrivals including (a) reflections used in conventional reverse time migration, (b) surface multiples, (c) internal multiples, (d) duplex-waves.

Numerical Results

DRTM is first demonstrated on a simple two layer synthetic data case with a near-surface velocity anomaly. Figure 3 shows the true velocity model. The lower layer has a velocity of 3000 m/s, and the upper layer has a velocity of 1500 m/s. The near-surface anomaly is 500 m/s. A shot gather located above the anomaly is displayed in Figure 4(a), and the direct arrival is shown in Figure 4(b). The conventional RTM image (Figure 5(a)), shows poor amplitude continuity on the sides of the anomaly as well as the reflector below compared with forward propagating the direct arrival, Figure 5(b).

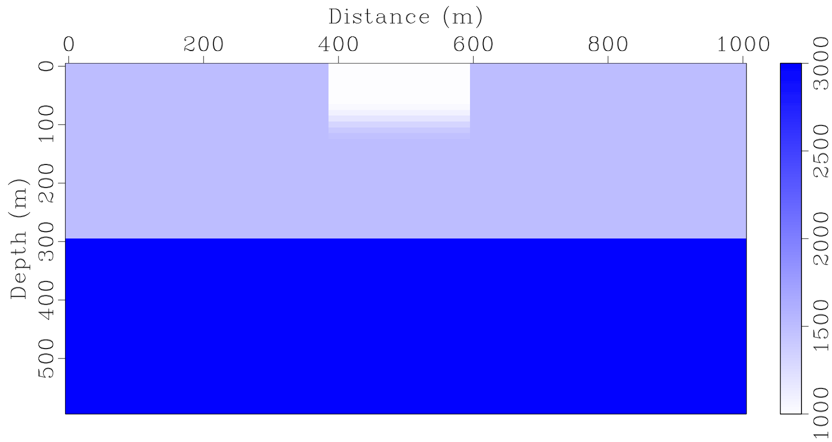

Figure 3– Velocity model with anomaly.

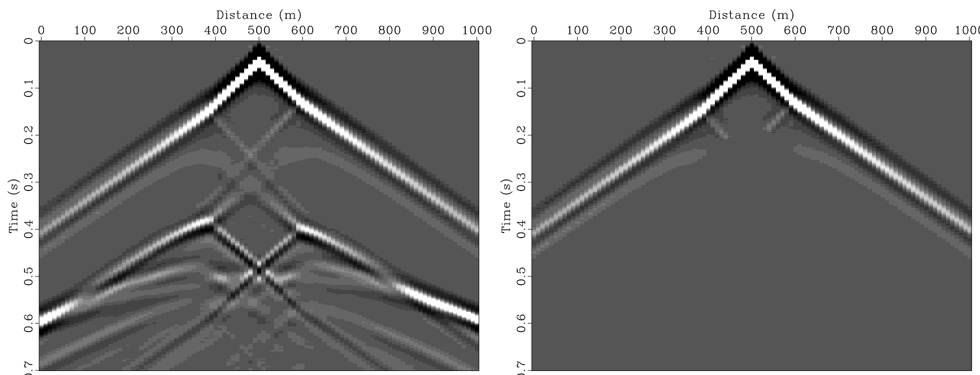

(a) **(b)**

Figure 4 – Data recorded from the synthetic model including (a) shot gather and (b) the direct arrival.

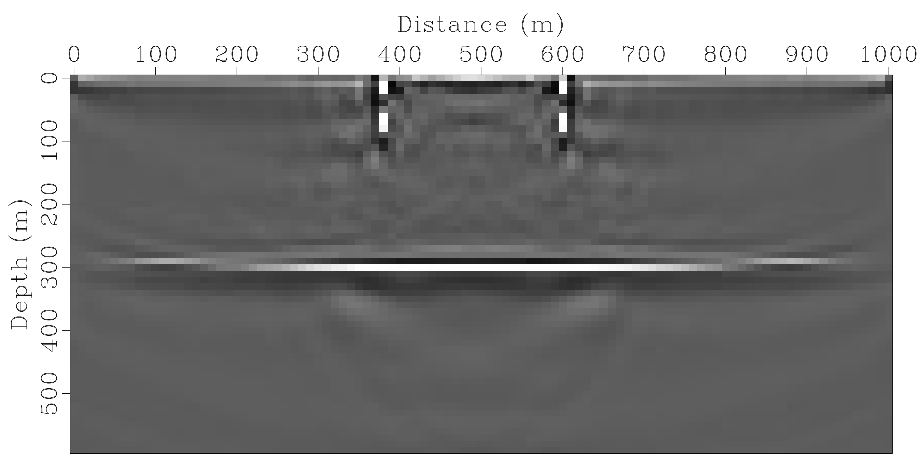

(a)

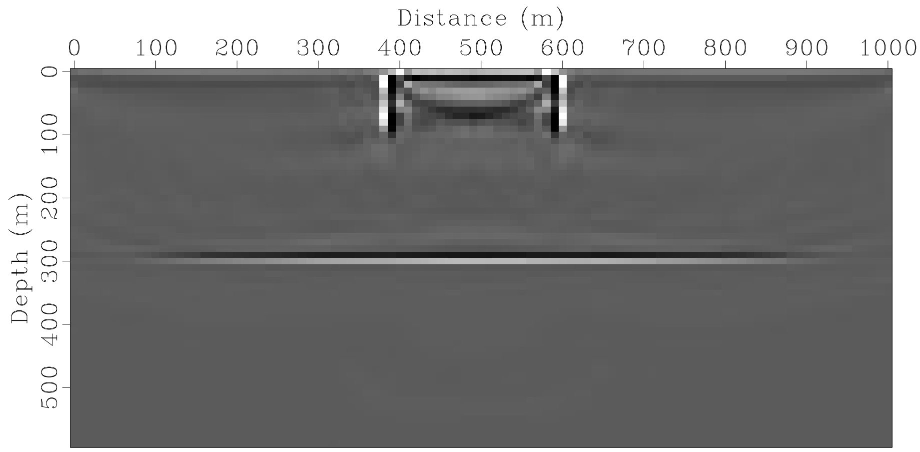

(b)

Figure 5 – Depth images from (a) conventional RTM and (b) DRTM.

Figure 6 shows a second model comprising two layers and multiple low velocity anomalies within the first layer. These anomalies have a fixed velocity of 1500 m/s. The upper layer has a velocity of 2000 m/s and the lower layer 3000 m/s. Shot records recorded using this model are shown in Figure 7(a), and the direct arrival is shown in Figure 7(b). Figures 8(a) and 8(b) show conventional RTM and duplex-wave depth migration images, respectively. Again, the RTM result shows poor imaging of the near-surface anomalies as well as uneven reflector amplitudes below compared to the DRTM image.

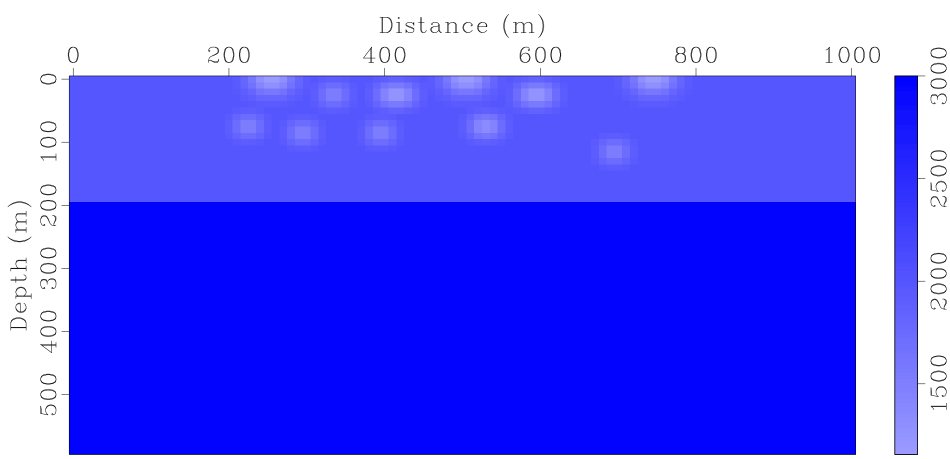

Figure 6 – Velocity model with scattered near-surface anomalies.

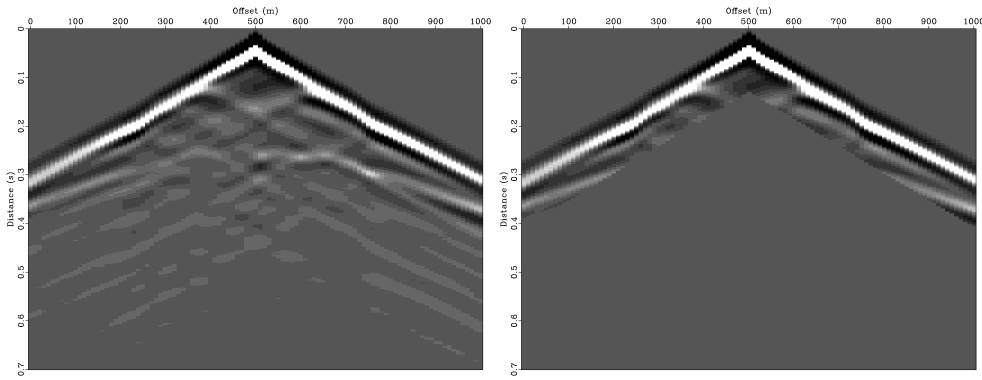

(a) **(b)**

Figure 7 – Data recorded from the second synthetic model including (a) shot gather and (b) the direct arrival.

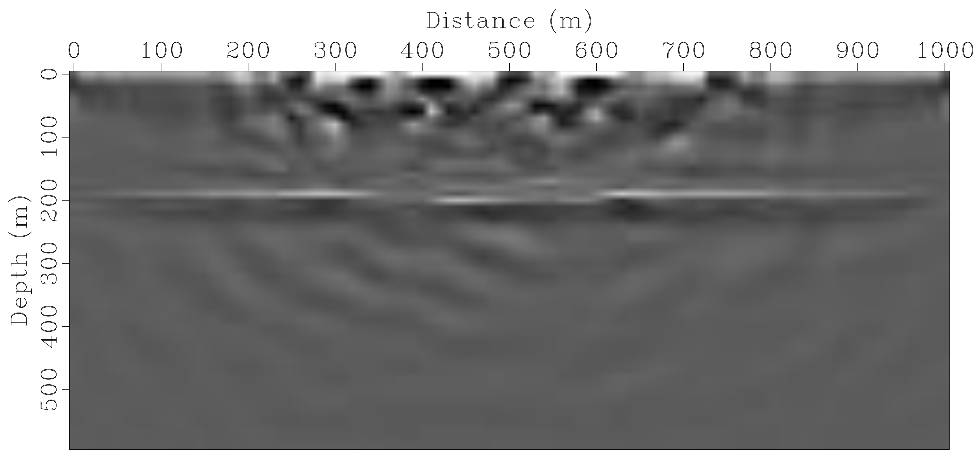

(a)

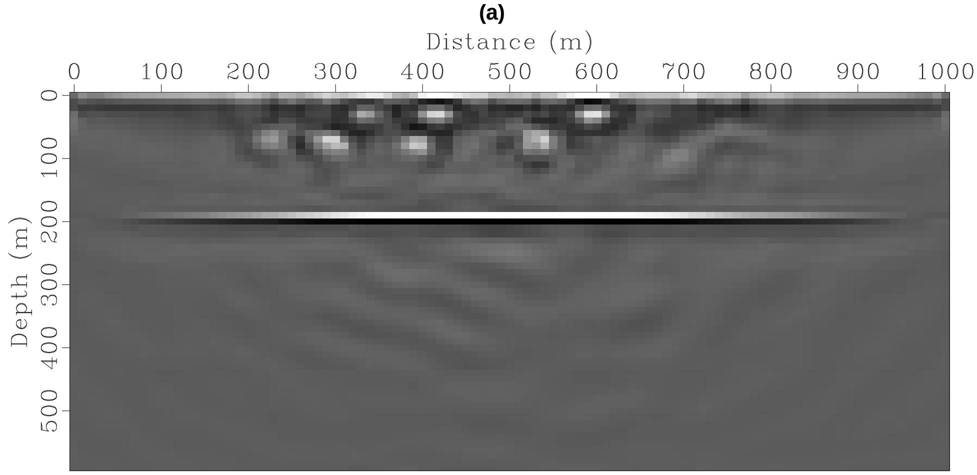

(b)

Figure 8 – Depth images including results from (a) conventional RTM, and (b) imaging using duplex-wave migration.

We next compare RTM and DRTM using portion of Marmousi model (Figure 9). Imaging is applied to data from the part of the smoothed Marmousi model shown in Figure 10. A shot gather and its direct arrival generated from the model are shown in Figures 11(a) and 11(b), respectively. The shot interval is 72 m, the receiver spacing is 24 m, and the record length is 2.9s. Figures 12(a), and 12(b) show depth images from RTM and DRTM, respectively, using the true velocity model. In contrast, RTM and DRTM images in Figures 13(a) and 13(b), respectively, are obtained using a smoothed Marmousi model. The smoothing radius is 72 m in both vertical and horizontal directions.

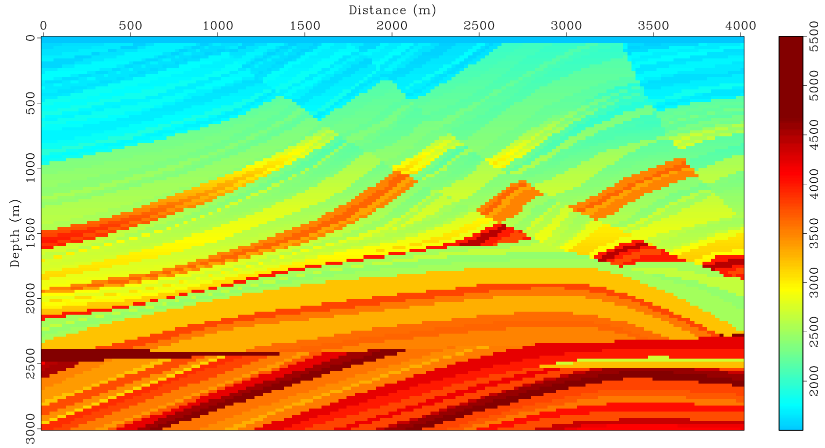

Figure 9 – portion of Marmousi model.

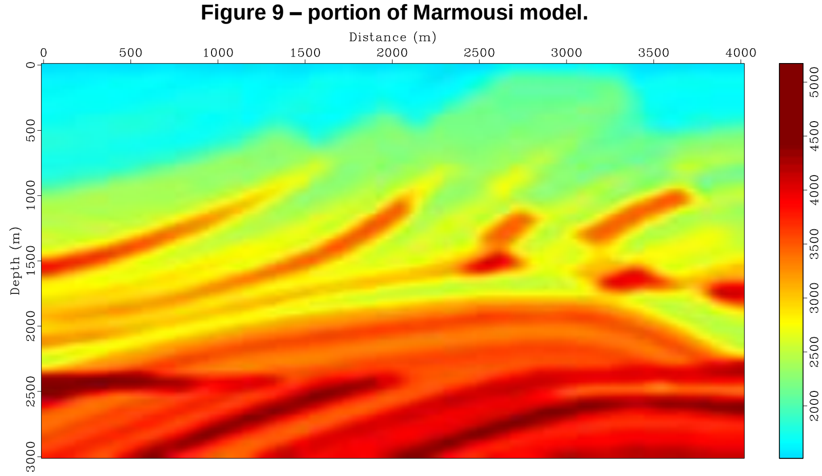

Figure 10 – Smoothed subset of the Marmousi model.

.

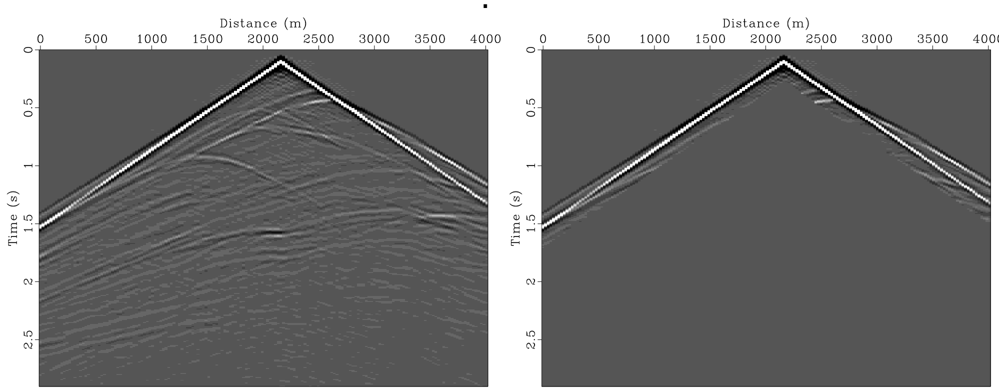

(a) **(b)**

Figure 11 – Data recorded from the Marmousi model including (a) shot gather and (b) the direct arrival.

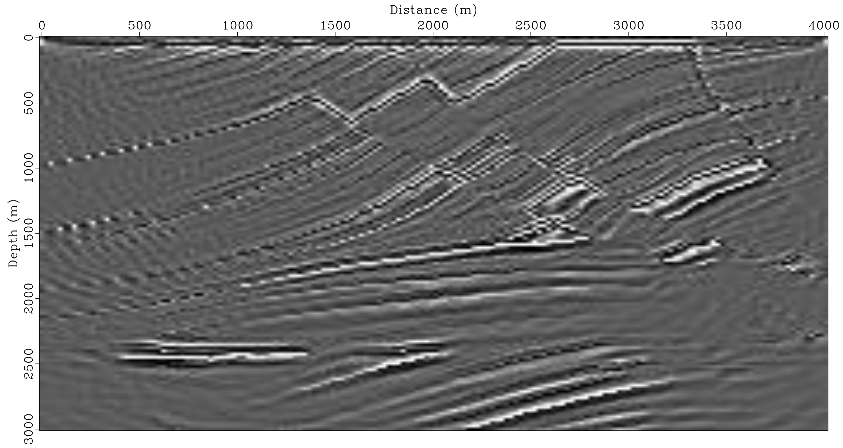

(a)

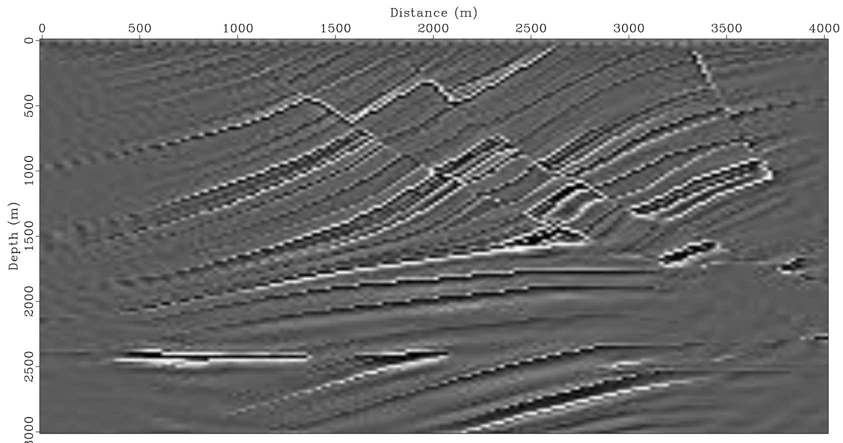

(b)

Figure 12 – Depth imaging results using Marmousi model from (a) conventional RTM and (b) duplex migration.

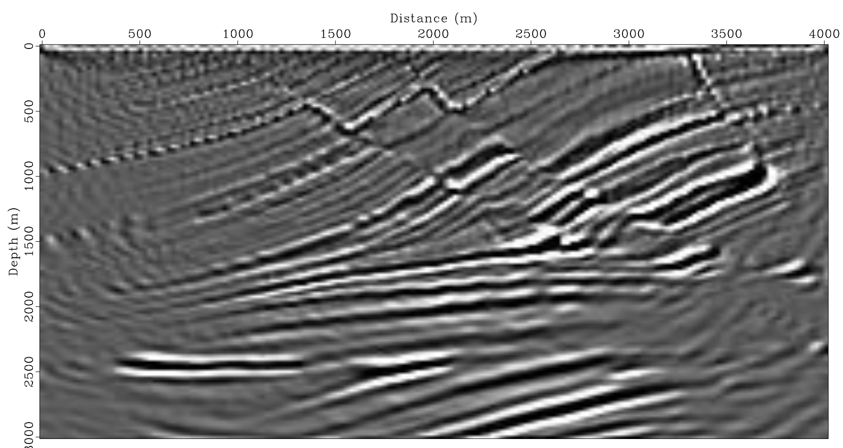

(a)

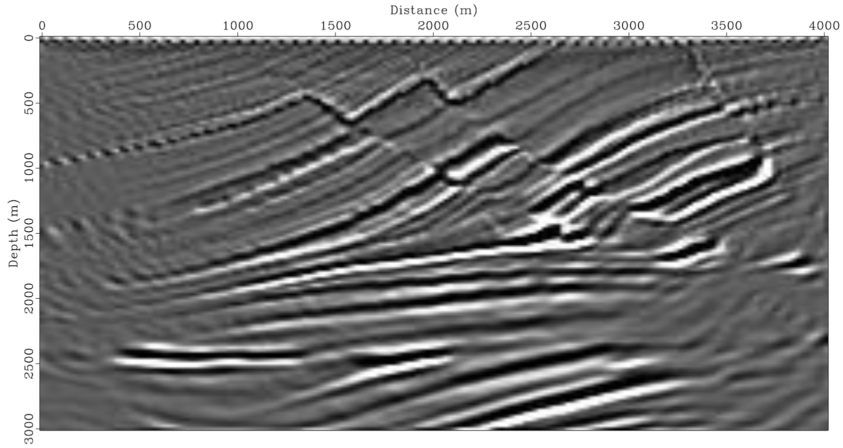

(b)

Figure 13 – Depth imaging results using a smoothed Marmousi model from (a) conventional RTM and (b) duplex migration.

Field tests

We apply DRTM to a 2-D onshore seismic data set comprising 400 shots with a receiver and source spacing of 25m. Figure 14 displays a portion of the migration velocity derived from migration velocity analysis (MVA). A transition zone 2-D shot gather is shown in Figure 15(a) and the direct arrival is shown in Figure 15(b). Results from conventional RTM and DRTM are shown in Figures 16(a) and 16(b), respectively. The DRTM result by forward extrapolating the direct arrival produces an enhanced image for complex near-surface structures compared to results from conventional RTM (Figure 16: shallow events marked by red arrows). In RTM, we use a conventional mathematical source (Ricker wavelet). We call it a singular source since it has a singularity called a coordinate singularity (Prochnow et al., 2017). With this mathematical source we can image the deeper area as shown in Figure 16(a). When using the direct arrival as a source in DRTM, the coordinate singularity at the physical source location is very weak (Figure 15b). Therefore, the deeper area is not clearly imaged in Figure 16(b).

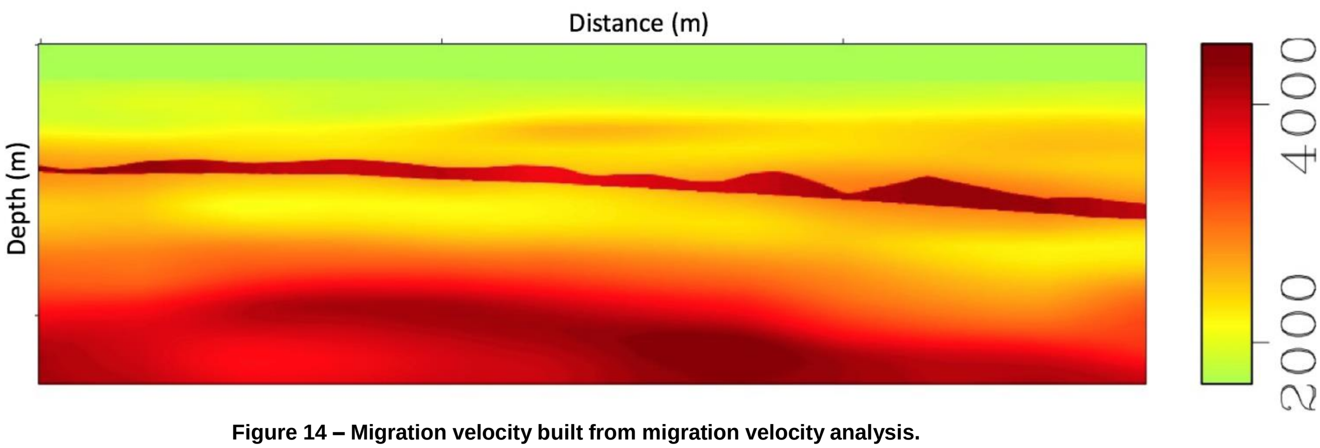

Figure 14 – Migration velocity built from migration velocity analysis.

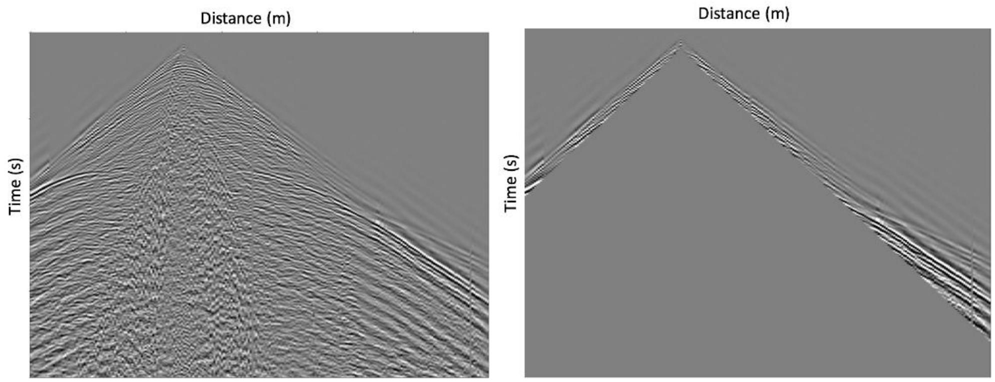

(a) (b)

Figure 15 – Field data including (a) a shot gather, and (b) the direct arrival after muting.

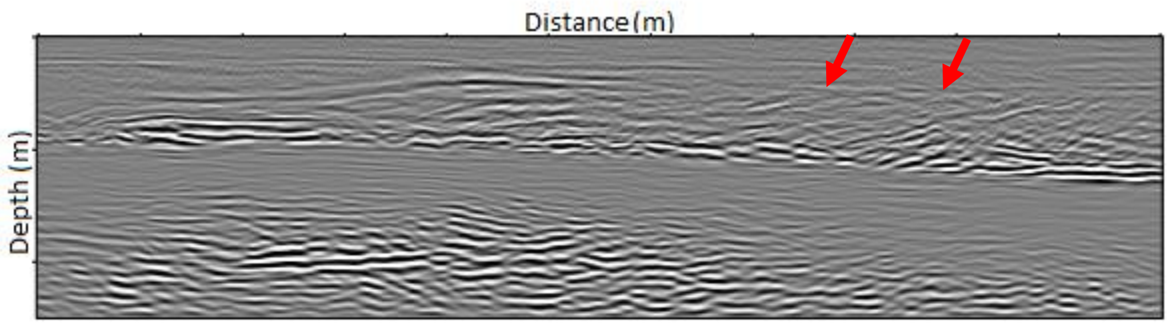

(a)

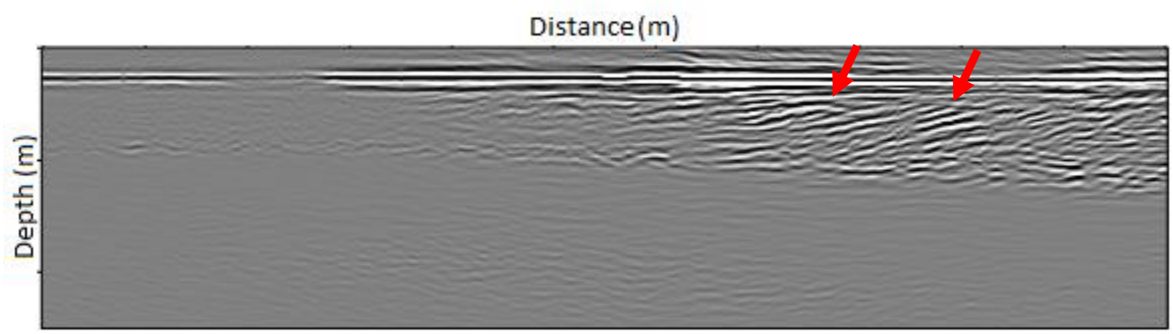

(b)

Figure 16 – Field data example showing depth images from (a) conventional RTM stack and (b) DRTM stack.

Wang et al. (2013b) proposed to replace the forward propagated source function for data-to-data RTM with a synthetic wavelet added to the recorded data. This approach enables the imaging of the free-surface related multiples and primaries simultaneously. Here, we adopt the approach of Wang et al. (2013b) to compensate for the weak signal at near-offset to get a better image in the deeper region. Figure 17 shows the direct arrival after amplifying the near-offset trace. We boost the source singularity by multiplying the source by a scaling factor. Using the near-offsets, the DRTM image (Figure 18) shows improvement in the deeper area compared to Figure 16(b). Figures 16(b) and 18 both show a relatively flat reflector at the surface, which is the acquisition footprint of the sources and the receivers.

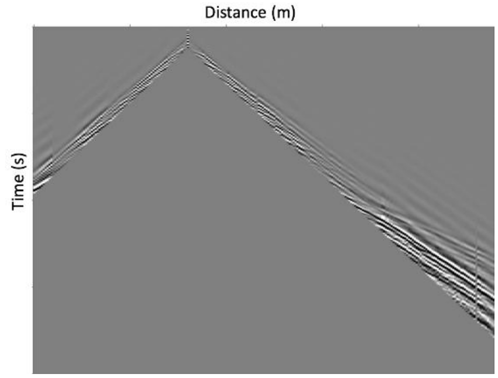

Figure 17 – Direct arrival after boost up the near-offset trace.

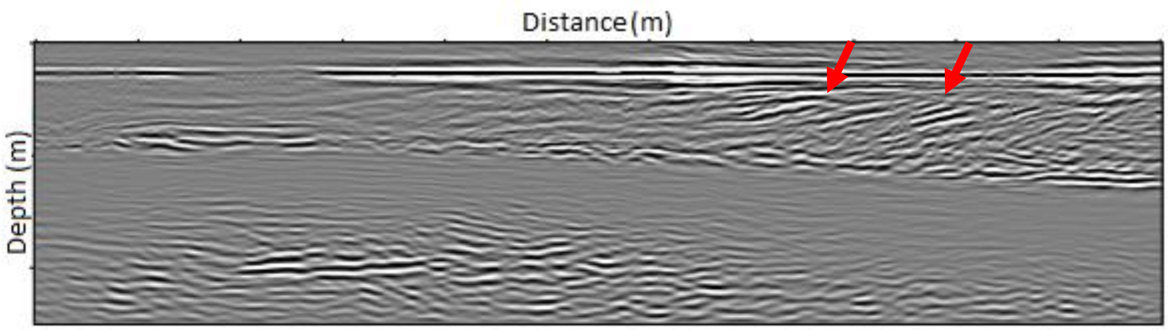

Figure 18 – DRTM image.

Conclusions

We developed a depth migration technique for imaging complex near-surface structures. The method uses duplex waves and produces an enhanced image for complex near-surface structures when compared to conventional imaging methods, which use only reflection data. The algorithm is based on forward propagating the direct arrivals, which shows better results than estimating the source in RTM. Forward propagating the direct arrivals is equivalent to reproducing the primary source for surface seismic data. The algorithm images better below near-surface anomalies when compared to the RTM algorithm, which neglects the near-surface scatterers in the velocity model. Also, the proposed algorithm can better resolve near-surface scatterers that are close to each other much better than RTM. Through numerical examples, we show that forward propagating the direct arrivals generates results comparable to conventional RTM. However, DRTM does require the near-offsets to be recorded. In particular, zero offsets must exist in the data. The DRTM method has been successfully demonstrated on a field dataset.

References

Alkhalifah, T., and M. Zuberi, 2011, Imaging by forward propagating the recorded data-an analysis: Presented at the *73rd EAGE Conference and Exhibition incorporating* SPE EUROPEC 2011.

Baysal, E., D. D. Koslo, and J. W. Sherwood, 1983, Reverse time migration: Geophysics, 48, 1514-1524.

Berkhout, A., and D. J. Verschuur, 1994, Multiple technology: Part 2, migration of multiple reflections, in *SEG Technical Program Expanded Abstracts* 1994: Society of Exploration Geophysicists, 1497-1500.

Davydenko, M., and D. Verschuur, 2017, Full-wavefield migration: using surface and internal multiples in imaging: Geophysical Prospecting, 65, 7-21.
Guitton, A., 2002, Shot-profile migration of multiple reflections, in *SEG Technical Program Expanded Abstracts* 2002: Society of Exploration Geophysicists, 1296-1299.
Kosloff, D. D., 1983, Migration with the full acoustic wave equation: Geophysics, 48, 677-687.
Kumar*, A., G. Blacquiere, and E. Verschuur, 2014, 3d acquisition geometry analysis: Incorporating information from multiples, in SEG Technical Program Expanded Abstracts 2014: Society of Exploration Geophysicists, 30-35.
Liu, Y., X. Chang, D. Jin, R. He, H. Sun, and Y. Zheng, 2011, Reverse time migration of multiples for subsalt imaging: Geophysics, 76, WB209-WB216.
Liu, Y., H. Hu, X.-B. Xie, Y. Zheng, and P. Li, 2015, Reverse time migration of internal multiples for subsalt imaging: Geophysics, 80, S175-S185.
McMechan, G. A., 1983, Migration by extrapolation of time-dependent boundary values: Geophysical Prospecting, 31, 413-420.
Muijs, R., J. O. Robertsson, and K. Holliger, 2007, Data-driven adaptive decomposition of multicomponent seabed seismic recordings: Application to shallow-water data from the North Sea: Geophysics, 72, V133-V142.
Prochnow, B., O. O'Reilly, E. M. Dunham, and N. A. Petersson, 2017, Treatment of the polar coordinate singularity in axisymmetric wave propagation using high order summation-by-parts operators on a staggered grid: Computers & Fluids, 149, 138-149.
Wang, Y., X. Chang, and H. Hu, 2013b, Simultaneous reverse time migration of primaries and free-surface related multiples without multiple prediction: Geophysics, 79, S1-S9.
Vershuur, D. J., and A. Berkhout, 1994, Multiple technology: Part 1, estimation of multiple reflections, in *SEG Technical Program Expanded Abstracts* 1994: Society of Exploration Geophysicists, 1493-1496.
Zhang, Y., G. Zhang, and J. Sun, 2007, Explicit marching method for reverse-time migration: *SEG Expanded Abstracts*, 23002303.
Zuberi, A., and T. Alkhalifah, 2013, Imaging by forward propagating the data: Theory and application: Geophysical Prospecting, 61, 248-267.